© 2000 The Chemical Society of Japan Bull. Chem. Soc. Jpn., 73, 795—800 (2000)

# Structure Sensitivity of Platinum Catalysts for Decomposition Reaction of Diluted NO

**Takeshi Furusawa and Ken-ichi Aika***

Interdisciplinary Graduate School of Science and Technology, Tokyo Institute of Technology,
4259 Nagatsuta, Midori-ku, Yokohama 226-8502

(Received May 25, 1999)

Decomposition reactions of diluted (0.1%) NO without reductants were studied over alumina supported platinum catalysts with various platinum loadings. Supported catalysts with different dispersions of platinum particle (different particle sizes) were prepared by controlling platinum loading on alumina. The XRD measurements disclosed that the relative peak intensity of (111) layer increased with an increase in the particle size, suggesting that the XRD peak intensity was closely related to the surface structure of platinum particles. The activities (TOF) of NO decomposition increased with an increase in the particle size or the peak intensity of (111) structure. Temperature programmed desorption (TPD) of oxygen was also studied on these samples. The temperature of oxygen desorption decreased with an increase in the particle size or the ratio of (111) structure. The NO decomposition was reasonably explained, as it preceded more easily on the (111) surface where oxygen was weakly adsorbed on platinum. It was also pointed out that the surface structure was more sensitive for oxygen adsorption than the NO decomposition reaction.

Removal of nitrogen oxide exhausted from automobiles is an important environmental issue. The three-way catalyst which eliminates $NO_x$, CO, and hydrocarbon is widely used for this purpose.[1] Among the elements used in the three-way catalyst, platinum is the most durable against catalyst poisons such as sulfur[2] and is the main active element. For these catalyst systems, NO decomposition is accelerated by the reductants such as CO and hydrocarbons through the redox mechanism on platinum. Platinum catalysts are also expected to be useful for the direct NO decomposition catalysts[3—9] without reductants or even under the excess oxygen.

Several investigations of direct NO decomposition over the platinum single crystal[7—9] have been reported. The reaction is affected by the surface structure. It is also known that the N–O bond dissociation step is the rate-determining of NO decomposition reaction, and Pt(100) is the most effective surface. This does not mean that Pt(100) is the most active surface under the steady state reaction condition where surface oxygen produced might change the situations. For supported rhodium catalysts,[10—13] it has been reported that NO reduction activities increase with an increase in particle size of rhodium metal. As for palladium catalysts,[14—16] it has also been reported that NO reduction activities are affected by surface structure and the Pd(111) surface is the most effective. To the author's knowledge, however, few NO decomposition studies have been carried out in view of the surface structural effect of supported "platinum" catalysts under the low NO concentration. It is important to analyze the structural effects of platinum-supported catalysts in order to obtain the fundamental information of NO decomposition under the environmental conditions. The purpose of this study is to examine the relation between platinum particle size and activities of NO decomposition and $O_2$ desorption, and to discuss it as related to the reaction mechanism and the surface structure.

## Experimental

Platinum particle size was controlled by changing the loading on alumina. γ-alumina (JRC-ALO-4) was impregnated with an aqueous solution of $H_2PtCl_6\cdot 6H_2O$ (Kanto Chemical Co., Inc.) and dried at 383 K overnight. After preparation, 0.5 g of catalysts were loaded in the reactor and treated with 400 Torr of $H_2$ (1 Torr = 133.322 Pa) at 573 K for 1 h. Hydrogen chemisorption was measured at 273 K for calculating the Pt dispersion, assuming H/Pt(s) = 1/1. The Pt particle diameter, $d$ (nm), was calculated by the following equation: $d = 1.13/f$, where $f$ means dispersion, Pt(s)/Pt(b) (the surface Pt atom number divided by the bulk Pt atom number).

Usually 0.2 g aliquots of catalysts were loaded in the reactor for the analysis of the reaction: NO decomposition. The catalysts were treated with 400 Torr of $H_2$ at 573 K for 1 h. NO decomposition was carried out at the temperature range of 823—923 K using 0.1% NO in He (at a flow rate of 60 ml min$^{-1}$), which is a typical concentration out of a burning gas. Effluent gases out of the reactor were analyzed with an on-line gas chromatograph (Hewlett–Packard 5890). Separation of the products was achieved on a Porapak Q and Molecular Sieve 5A.

For the $O_2$-TPD experiments, 0.5 g aliquots of catalysts were loaded in the quartz reactor and treated with $H_2$ (30 ml min$^{-1}$ at 573 K for 1 h), followed by evacuation at the same temperature for 1 h, and finally cooled to 298 K. Adsorption of $O_2$ was performed at 298 K under atmospheric $O_2$ flow (30 ml min$^{-1}$), then gaseous $O_2$ was removed by evacuation. The catalyst temperature was then increased up to 923 K at the rate of 6 K min$^{-1}$ and the desorbed gas (mass number 32) was qualitatively analyzed using a quadrupole mass spectrometer.

XRD of untreated samples were measured in order to obtain the structural data, which may be related with the Pt surface structure. Cullity has reported that only X-ray diffraction beams from the surface and subsurface can be detected for samples which strongly absorb X-rays, such as tungsten.[17] Platinum, which has a higher atomic number than tungsten, is considered to absorb X-rays strongly, too. The peak intensity for every structural index is rationalized by referring to the calibration factor (ASTM).

## Results and Discussion

Figure 1 shows the dependency of Pt loading of $Pt/Al_2O_3$ on the dispersion and the particle size. It is found that the dispersion decreases with an increase in Pt loading of $Pt/Al_2O_3$, and that the particle size increases with it. These results are generally accepted[18] and are in good agreement with results of supported rhodium catalysts presented by Kasper et al.[10] and Oh et al.,[12] and with those of palladium catalysts presented by Rainer et al.[16]

Figure 2 shows the time course of effluent gases during the NO decomposition at 923 K over 1.97 wt% $Pt/Al_2O_3$ as an example. It was found that the unreacted NO concentration increased and $N_2$ concentration first decreased with time and became constant after 50 min. This indicates that the catalyst is rapidly deactivated to some level and then stabilized. It is also shown that $O_2$ is not observed initially and the concentration first increases with time and then becomes constant after 50 min. This behavior indicates that small amounts of oxygen atoms are strongly adsorbed and create a strong inhibition of the platinum catalysis. $N_2O$ and $NO_2$ are usually thought of as by-products. $N_2O$, which should be detected easily, was not observed. $NO_2$, of which the quantity is hard to determine, was observed by GC. Thus, the authors first calculated $NO_2$ concentration from the shortage of total concentration of nitrogen atoms. Then, the amounts of adsorbed oxygen atoms were calculated by subtracting the $NO_2$ concentration from the shortage of total concentration of oxygen atoms. It was estimated that the amount of adsorbed oxygen atoms on catalyst during the reaction was 0.8 monolayer of surface platinum atoms. Adsorbed oxygen atoms are well known to inhibit the reaction.[3,4] Oxygen atoms strongly adsorbed on platinum are difficult to desorb from the surface active site for NO decomposition. Figure 2 also shows the time courses of total (observable) amounts of nitrogen atoms and oxygen atoms. It is seen that both nitrogen atoms and oxygen atoms increase with time initially and then become constant; the observed amount of oxygen atoms is always smaller than that of nitrogen atoms. This indicates the production of $NO_2$ as a side reaction, although this could not be determined by the present analytical method (GC).

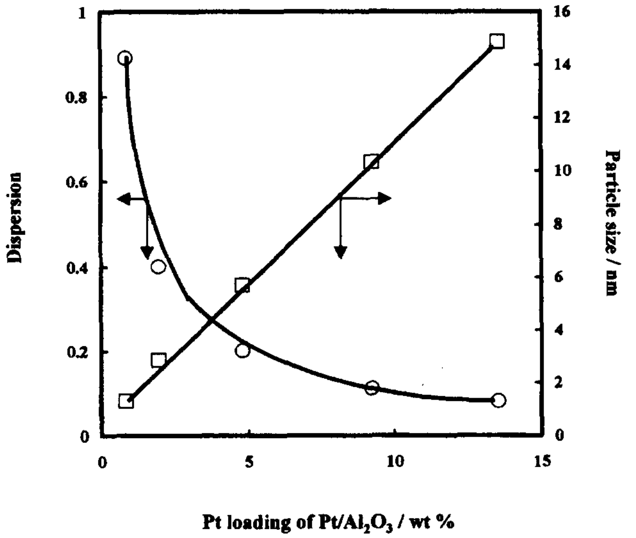

Fig. 1. Dependency of Pt loading of $Pt/Al_2O_3$ on the dispersion (○) and the particle size (□).

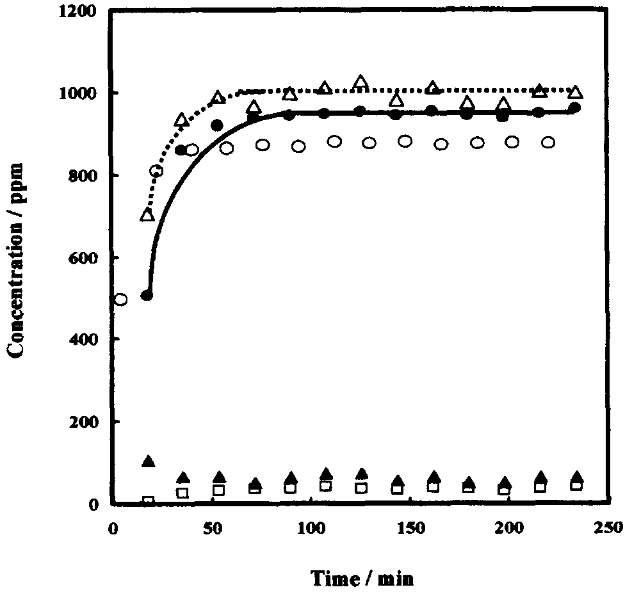

Fig. 2. Time course of effluent gas concentration during the decomposition reaction. NO (1030 ppm) was introduced over 1.97 wt% $Pt/Al_2O_3$ at 923 K; ○: NO, ▲: concentration of $N_2$ molecule, □: concentration of $O_2$ molecule, ···△···: total concentration of N atom, and —●—: total concentration of O atom.

$$NO \rightarrow N(a) + O(a) \quad (1)$$

$$N(a) + N(a) \rightarrow N_2 \quad (2)$$

$$O(a) + O(a) \rightarrow O_2 \quad (3)$$

$$O(a) + NO \rightarrow NO_2 \quad (4)$$

Reaction (2), produced nitrogen, was measured directly from GC data, but, reaction (4) was estimated from the above method. The ratio of the two reactions (2) and (4) is estimated as 5 to 3.

Figure 3 shows XRD patterns of various loading amounts (0.87 wt%, 1.97 wt%, 4.81 wt%, 9.25 wt%, 13.54 wt%) of $Pt/Al_2O_3$ after the reaction using Cu$K\alpha$ as the X-ray source. Three major peaks at 40, 46, and 67 degree for $2\theta$ are identified as Pt(111), Pt(200), and Pt(220), respectively. These are corresponding to (111), (100), and (110) layers. The intensity of Pt(111) surface increases with an increase in Pt loading of $Pt/Al_2O_3$, comparing with Pt(200) and Pt(220). The (111) layers are well developed at large particles of Pt.

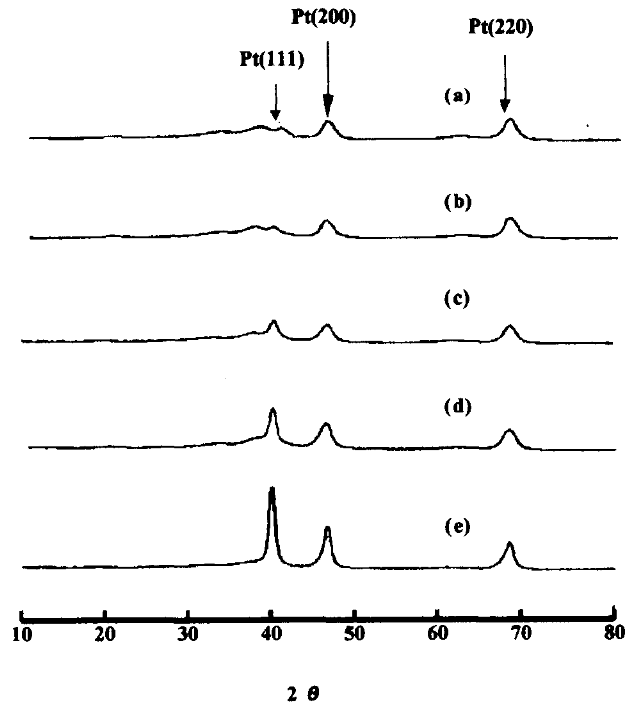

Fig. 3. XRD patterns of $Pt/Al_2O_3$ after the reaction using Cu$K\alpha$ as X-ray source; (a) 0.87 wt%, (b) 1.97 wt%, (c) 4.81 wt%, (d) 9.25 wt%, and (e) 13.54 wt% $Pt/Al_2O_3$.

The intensity deference in layers has also been reported for Pd catalysts.[19] The contribution of main layer indices are calculated by the observed peak intensity and the calibration factor, and shown as a function of Pt loading of $Pt/Al_2O_3$ in Fig. 4. The ratio of Pt(111) layer increases with an increase in Pt loading of $Pt/Al_2O_3$. Pt(200) layer seems to be rather constant, while Pt(220) seems to be decreased.

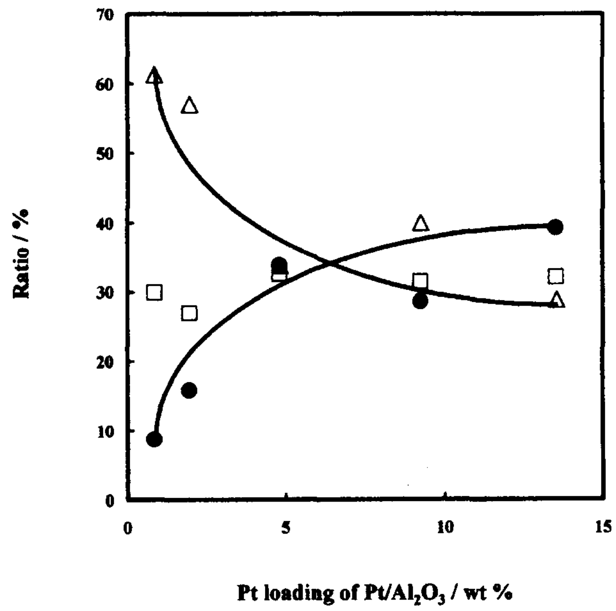

Fig. 4. Relation between the XRD peak intensity of major layer and Pt loading of $Pt/Al_2O_3$; ●: Pt(111), □: Pt(200), and △: Pt(220).

If the particle is spherical, the dense surface or high coordination surface atom such as (111) increases with an increase in particle size, which is in agreement with the general theory.[18,20] When platinum loading is high, platinum particle size is large and the coordination number of a surface atom is high. Even though XRD measurements are thought to be surface-sensitive in some extent, however, the change of XRD in Fig. 4 seems to be extraordinary. The authors suppose that particle crystal shape may be different at the high loading or the large particle size. Wang et al. have proposed a model of platinum particle of a well-developed crystal. Figure 5 shows such model structures reproduced from Wang's paper.[21] The (111) surface has the smallest surface energy among (111), (100), and (110) surfaces[22] and the second is the (100) surface. So we suppose that the structure with developed (111) layer is likely to have (111) surface. Now, it is suggested that large particles prefer the cubo-octahedron (Fig. 5a) or spheres; however, smaller particles prefer cubes (Fig. 5b) under the reaction condition. Smaller particles cannot make much (111) surface because the surface atoms must have a lower coordination number. For such cases, (100) surface must prevail, where the particle shape is slightly unstable. In this case, oxygen adsorption stabilizes the unstable cube structure of small particles. Oxygen is thus considered to be adsorbed more strongly on (100) than on (111). Similar results have been reported by Xu et al.[23] using IR techniques in the case of $Pd/SiO_2$ (film). Palladium evaporated onto a silica thin film has been claimed to possess (111) and (100) facets from the results that adsorption states of NO and CO

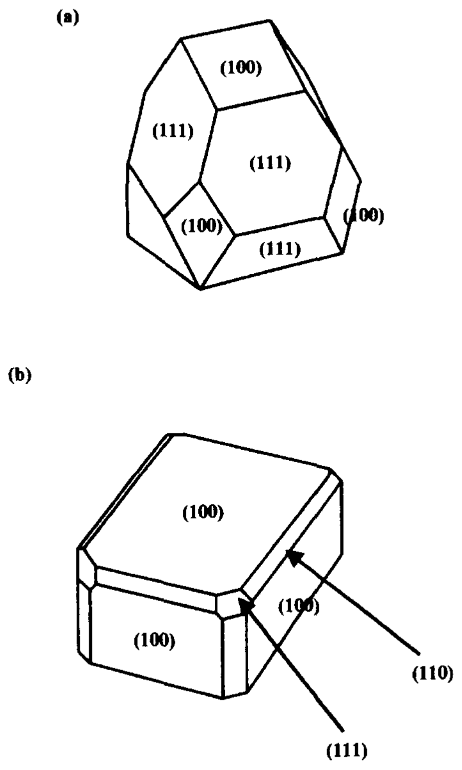

Fig. 5. The model shapes of Pt particles on $Al_2O_3$. (a) cubo-octahedron, (b) cubes.

reflect the surface structure. They have compared the adsorption state of CO and NO on such palladium catalysts with those on the single crystal surface. Altman et al.[24,25] have also reported that (111) surface structure prevails with increase in platinum vapor exposure in the case of $Pt/Al_2O_3$. They evaporated platinum on both amorphous alumina and $\alpha$-$Al_2O_3\{0001\}$ crystal, and found that CO desorption temperature from two catalysts was close to that from Pt(111) single crystal when platinum particle size was well developed.

The steady state rates of NO decomposition at 823, 873, and 923 K were measured on various catalysts. The turnover frequency (decomposed NO molecules/surface Pt/s) is plotted as a function of particle size in Fig. 6. The TOFs generally increase with the particle size. The TOF is also plotted as a function of (111) facet intensity of platinum in Fig. 7. The activities of NO decomposition increase with an increase in the ratio of Pt(111) surface. Some structure sensitivity is observed, but the extent is not as remarkable as in the case of reduction of NO on Rh particles.[26]

In the case of rhodium catalysts, Penden et al.[13] have compared the NO+CO reaction on Rh(111) surface and on Rh(110) surface. Rh(110) surface showed higher selectivity to $N_2$ (vs. to $N_2O$) than Rh(111) surface. They have explained that on Rh(110) surface NO dissociates more easily than on Rh(111), and the recombination of N atoms preferentially proceed compared to NO+N reaction.[27,28] This is an example of structure sensitivity to NO reaction, although it contains reduction with CO and the reaction was not analyzed in the steady state.

In the case of palladium catalyst, Rainer et al.[16] reported that Pd(111) surface is more active than Pd(110) or Pd(100) surface for the steady state reaction of NO with CO. They have explained that Pd(100) face is more active for NO dissociation, but nitrogen atoms that are produced from dissociation are stabilized on the surface and inhibit the reaction. Vesecky et al.[14] have supported their conclusion. Rainer et al. also studied the conventional $Pd/Al_2O_3$ catalysts for the same reaction and explained the higher activities on larger particles with similar reasons.

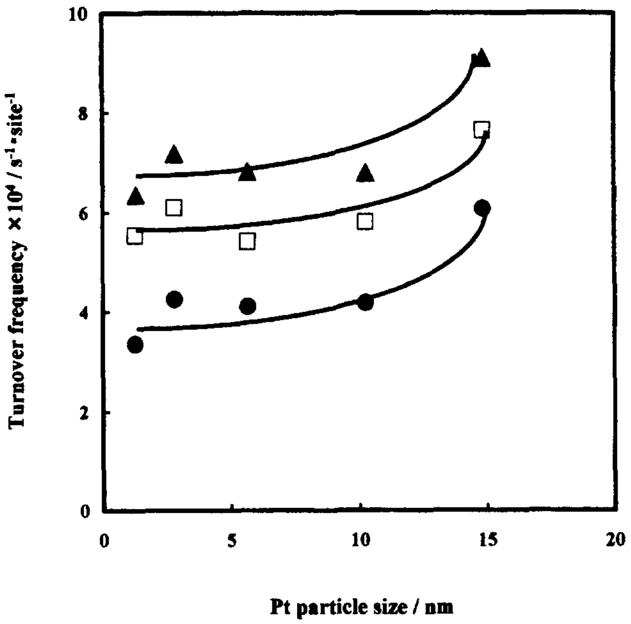

Fig. 6. Turnover frequency of NO decomposition on Pt surface as function of the Pt particle size at various reaction temperature ●: 823 K, □: 873 K, and ▲: 923 K.

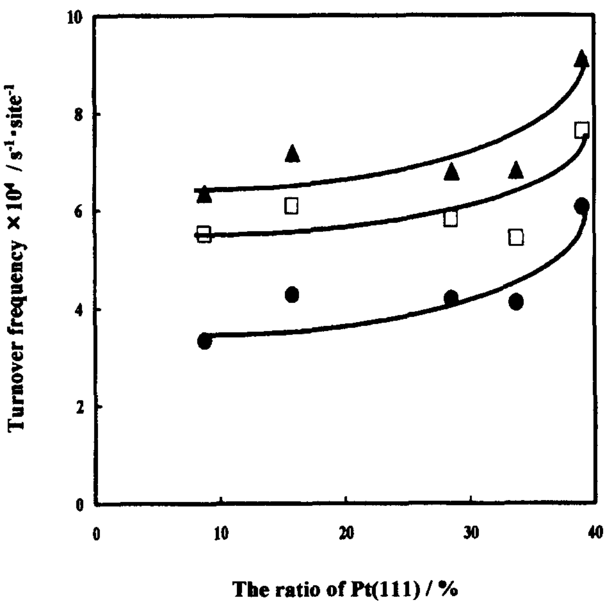

Fig. 7. Turnover frequency of NO decomposition on Pt surface as function of the Pt(111) ratio at various reaction temperature ●: 823 K, □: 873 K, and ▲: 923 K.

Here, we supposed that Pt(100) surface is more active for NO dissociation but may stabilize oxygen atoms more strongly and give lower activities, whereas Pt(111) face is not facile for NO dissociation but desorption of oxygen atoms is considered to be much easier than on Pt(110), Pt(100) surface. This may explain the results that activities of NO decomposition increase with an increase in the ratio of Pt(111) surface.

Now, oxygen desorption was studied on our supported catalysts. Figure 8 shows the $O_2$ TPD profiles from various catalysts. The shapes of profiles were similar for various catalysts with one strong peak, which covered a wide temperature range. We paid attention to the peak top for every sample. Here, $O_2$ desorption temperatures were plotted as a function of particle size (Fig. 9) and of the ratio of Pt(111) surface (Fig. 10). $O_2$ desorption temperatures clearly decrease with an increase in the particle size and an increase in the intensity of Pt(111) surface. This behavior indicates that the closely packed Pt(111) surface structure keeps oxygen atoms weakly because of the high coordination of Pt atoms in the (111). Pt(110), Pt(100) surfaces that have lower coordination numbers can combine with oxygen strongly. Weinberg et al.[29] and Ducros et al.[30] have reported that $O_2$ initial sticking probability is 0.05 and 0.4 over Pt(111) and Pt(110) face, respectively. Gland et al.[31] have reported that $O_2$ initial sticking coefficient is 0.4 over Pt(s)-12(111)×(111) surface.

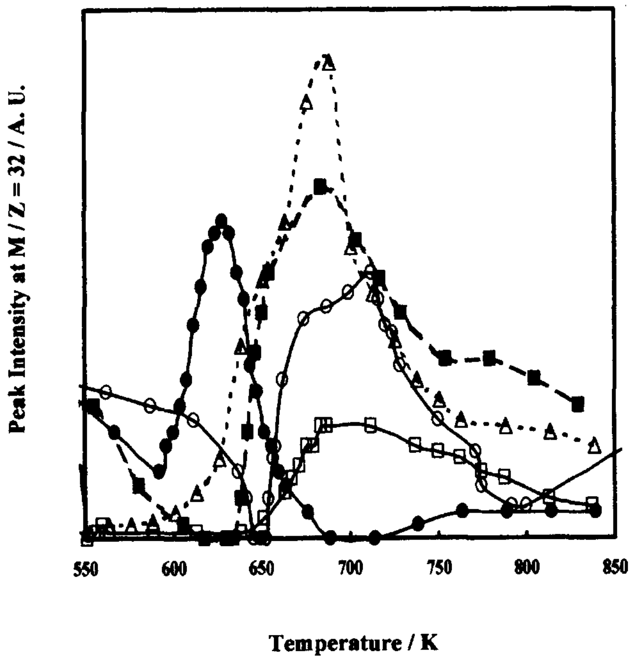

Fig. 8. TPD of oxygen from 0.87 wt% (○), 1.97 wt% (■), 4.81 wt% (△), 9.25 wt% (□), and 13.54 wt% (●), Pt/$Al_2O_3$ catalysts after $O_2$ pretreatment at 298 K for 1 h.

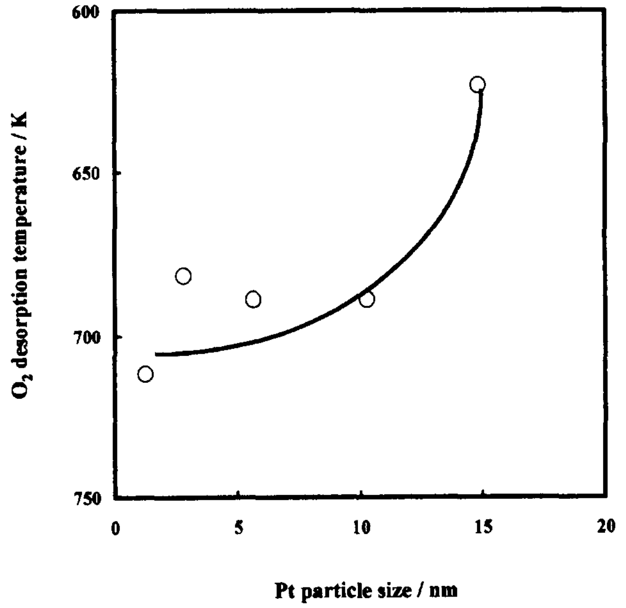

Fig. 9. The relation between Pt particle size and $O_2$ desorption temperature measuring from $O_2$–TPD.

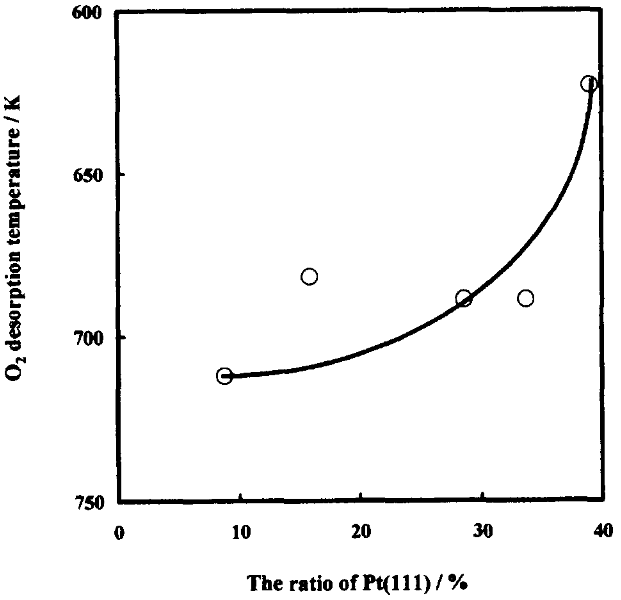

Fig. 10. The relation between the ratio of Pt(111) and $O_2$ desorption temperature measuring from $O_2$–TPD.

In the introduction, we pointed out that the N–O bond dissociation step was the rate-determining step of NO decomposition and that the Pt(100) surface was the most active surface. In this discussion, the adsorbed oxygen effect was ignored, though it must be important in the steady state. In this study, we have found that the activities (TOF) of decomposition increased with an increase of the particle size or the ratio of Pt(111) surface, but the extent was rather small. NO dissociation must be the rate-determining step and it may be fastest on Pt(100), the roughest surface claimed so far. However, under the steady state reaction, oxygen inhibits the active site and can control the reaction more. When the catalyst has large particle size or high ratio of Pt(111) surface, the catalyst must be more active because of the weak adsorption of oxygen atoms. This may be the reason why Pt(111) is the most active, though the extent is not so remarkable.

## Conclusion

We found that platinum particle size increased with an in increase of platinum loading of Pt/$Al_2O_3$ and that the ratio of Pt(111) surface also increased with an increase of platinum particle size. The activities of NO decomposition (TOF) increase with an increase in the ratio of Pt(111) layer. It was also found that $O_2$ desorption temperature decreased with an increase in the ratio of Pt(111) layers. Pt atoms on the Pt(111) layer have high coordination numbers and must adsorb oxygen atoms weakly, giving more vacant sites for NO decomposition. However the difference of activities was rather small. Probably the NO decomposition step itself is slower on Pt(111) compared with the speed on Pt(100). For the steady rate of NO decomposition, we must consider both factors and oxygen adsorption.

## References

1 J. W. Hightower and D. A. Van Leisberg, "Current Status of the Catalytic Decomposition of NO," in "The Catalytic Chemistry of Nitrogen Oxides," ed by R. L. Klimish and J. G. Larson, Plenum Press, New York (1975), p. 63.

2 T. Wang, A. Vazquez, A. Kato, and L. D. Schmidt, *J. Catal.*, **78**, 306 (1982).

3 R. R. Sakaida, R. G. Rinker, Y. L. Wang, and W. H. Corcoran, *A. I. Ch. E. J.*, **1961**, 658.

4 M. Shelef, K. Otto, and H. Gandhi, *Atmosp. Environ.*, **3**, 107 (1969).

5 A. Amirnazmi and M. Boudart, *J. Catal.*, **39**, 383 (1975).

6 H. P. Bonzel, G. Broden, and G. Pirug, *J. Catal.*, **53**, 96 (1978).

7 H. P. Bonzel and G. Pirug, *Surf. Sci.*, **62**, 45 (1977).

8 J. L. Gland and B. A. Sexton, *Surf. Sci.*, **94**, 355 (1980).

9 R. J. Gorte, L. D. Schmidt, and J. L. Gland, *Surf. Sci.*, **109**, 367 (1981).

10 J. Kaspar, C. de. Leitenburg, P. Fornasiero, A. Trovarelli, and M. Graziani, *J. Catal.*, **146**, 136 (1994).

11 Se. H. Oh, G. B. Fisher, J. E. Carpenter, and D. W. Goodman, *J. Catal.*, **100**, 360 (1986).

12 Se. H. Oh and C. C. Eickel, *J. Catal.*, **128**, 526 (1991).

13 C. H. F. Peden, D. N. Belton, and S. J. Schmieg, *J. Catal.*, **155**, 204 (1995).

14 S. M. Vesecky, D. R. Rainer, and D. W. Goodman, *J. Vac. Sci. Technol. A*, **14**, 1457 (1996).

15 S. M. Vesecky, P. Chen, X. Xu, and D. W. Goodman, *J. Vac. Sci. Technol. A*, **13**, 1539 (1995).

16 D. R. Rainer, S. M. Vesecky, M. Koranne, W. S. Oh, and D. W. Goodman, *J. Catal.*, **167**, 234 (1997).

17 B. D. Cullity, in "Elements of X-Ray Diffraction," Addison-Wesley Publishing Co., Inc., Reading, Massachusetts, U. S. A., (Japanese version, Agune Co., Tokyo (1978)), p. 130.

18 J. R. Anderson, in "Structure of Metallic Catalysts," Academic Press, London, (1975), p. 361.

19 N. Amemiya and S. Naito, *Shokubai* (*Catalysis*), **38**, 386 (1996).

20 R. Van Hardeveld and F. Hartog, *Surf. Sci.*, **15**, 189 (1969).

21 T. Wang, C. Lee, and L. D. Schmidt, *Surf. Sci.*, **163**, 181 (1985).

22 G. Wulff, *Z. Kristallogr. Mineral.*, **34**, 449 (1901).

23 X. Xu, P. J. Chen, and D. W. Goodman, *J. Phys. Chem.*, **98**, 9242 (1994).

24 E. I. Altman and R. J. Gorte, *Surf. Sci.*, **172**, 71 (1986).

25 E. I. Altman and R. J. Gorte, *J. Catal.*, **110**, 191 (1988).

26 H. C. Yao, Y. -F. Yu Yao, and K. Otto, *J. Catal.*, **56**, 21 (1979).

27 R. J. Baird, R. C. Ku, and P. Wynblatt, *Surf. Sci.*, **97**, 346 (1980).

28 T. W. Root, G. B. Fisher, and L. D. Schmidt, *J. Chem. Phys.*, **85**, 4687 (1986).

29 W. H. Weinberg, R. M. Lambert, C. M. Comrie, and J. W. Linnett, in "Proc. 5th Intern. Congr. on Catalysis," 1972, ed by J. Hightower.

30 R. Ducros and R. P. Merrill, *Surf. Sci.*, **55**, 227 (1976).

31 J. L. Gland, *Surf. Sci.*, **93**, 487 (1980).